Lithium fluoride thin film detectors for low-energy proton beam diagnostics by photoluminescence of colour centres

R.M. Montereali[1], A. Ampollini[1], L. Picardi[1], C. Ronsivalle[1], F. Bonfigli[1], S. Libera[1], E. Nichelatti[2], M. Piccinini[1], M.A. Vincenti[1]
[1]ENEA C.R. Frascati, Fusion and Technologies for Nuclear Safety and Security Department, Via E. Fermi 45, 00044 Frascati (Rome), Italy
[2]ENEA C.R. Casaccia, Fusion and Technologies for Nuclear Safety and Security Department, Via Anguillarese 301, 00123 S. Maria di Galeria (Rome), Italy
e-mail: rosa.montereali@enea.it

Abstract. Optically transparent LiF thin films thermally evaporated on glass and Si(100) substrates were used for advanced diagnostics of proton beams of energies from 1.4 to 7 MeV produced by a linear accelerator for protontheraphy under development at ENEA C.R. Frascati. The proton irradiation induces the formation of stable colour centres, among them the aggregate F_2 and F_3^+ optically active defects. After exposure of LiF films grown on glass perpendicularly to the proton beams, their accumulated transversal spatial distributions were carefully measured by reading the latent two-dimensional (2-D) fluorescence images stored in the LiF thin layers by local formation of these broad-band visible light-emitting defects with an optical microscope under blue lamp excitation. Taking advantage from the low thickness of LiF thin films and from the linear behaviour of the integrated F_2 and F_3^+ photoluminescence intensities up to the irradiation fluence of ~$5x10^{15}$ p/cm^2, placing a cleaved LiF film grown on Si substrate with the cutted edge perpendicular to the proton beam, the 2-D fluorescence image of the film surface could allow to obtain the depth profile of the energy released by protons, which mainly lose their energy at the end of the path.

1. Introduction

Luminescence properties of point defects in insulating materials are successfully used for solid state light sources and dosimeters. Among them, broad-band light-emitting F_2 and F_3^+ colour centres (CCs) in lithium fluoride, LiF, are well known for their application in tuneable lasers, miniaturised light sources and radiation imaging detectors [1]. Under blue optical pumping in their overlapping absorption bands, their efficient, broad photoluminescence (PL) spans the green-red visible spectral range. Versatile LiF thin-film radiation imaging detectors exploiting the peculiar spectral characteristics of F_2 and F_3^+ defects (two electrons bound to two and three close anion vacancies, respectively) and the radiation sensitivity of the LiF material have been proposed and successfully applied for extreme ultraviolet [2], soft and hard X-ray imaging [1].

The F_2 and F_3^+ laser-active CCs in LiF possess almost overlapping absorption bands peaked around 450 nm, called M band [3]; under light excitation in this spectral range they emit broad PL bands peaked at ≅ 678 nm and ≅ 541 nm, respectively [4], whose intensities can be detected by an optical microscope operating in fluorescence mode. Among the main peculiarities of the luminescent LiF-film solid-state radiation imaging detectors, noteworthy ones are their very high intrinsic spatial resolution, and wide dynamic range. Moreover, due to the stability of F_2 and F_3^+ CCs at room temperature (RT) in LiF, they are quite easy to handle, as insensitive to ambient light.

Recently, their use has been successfully tested for low energy proton beam advanced diagnostics [5,6]. In recent years, the use of hadrons in oncological radiotherapy has seen a remarkable growth because of the excellent ballistic properties of the heavy particles, which lose their energy at the end of the path in tissue, called Bragg peak, with a modest lateral diffusion, preserving the surrounding healthy organs during tumor irradiation. For energies higher than 1 MeV, protons traversing insulating materials lose their energy primarily through ionization and excitation of atoms [7]. Optically transparent LiF thin films thermally evaporated on amorphous and crystalline substrates [8] were used

for direct detection of proton beams of energy from 2 to 7 MeV produced by a linear accelerator for protontherapy under development at ENEA C.R. Frascati [9]. The proton irradiation of LiF films induces the local formation of stable CCs, mainly the primary F centres and the aggregate F_2 and F_3^+ ones [5,6].

After exposure of LiF films grown on glass substrates perpendicularly to the proton beams, their accumulated transversal spatial distributions were measured by reading with a conventional optical microscope the latent two-dimensional (2-D) fluorescence images stored in the LiF thin layers by local formation of optically active CCs at irradiation fluence in the range 10^{11}-10^{15} p/cm^2 [5,6].

Placing a cleaved LiF film grown on a Si(100) substrate [8] with the cut edge perpendicular to the proton beam direction, so that the film surface is parallel to the direction of the impinging particles, the 2-D fluorescence images could allow to obtain the depth profile of the energy released by protons, which mainly lose their energy at the end of the path [10,11].

Preliminary experimental results are reported. They show a qualitative agreement with the SRIM (The Stopping and Range of Ions in Matter) software simulations [12], taking into account the polycrystalline nature of the LiF films.

2. Materials and Methods

Exposed samples were polycrystalline LiF thin films, ≅0.8 μm thick, grown by thermal evaporation [8] on glass and Si(100) substrates kept at a constant temperature of 300°C during the deposition process, performed in a vacuum chamber at a pressure below 1 mPa, at ENEA Frascati. The starting material consists of LiF microcrystalline powder (Merck Suprapur, 99.99% pure), heated at about 840°C in a water-cooled tantalum crucible. The evaporation rate, monitored in situ by an INFICON quartz oscillator, was automatically controlled at a fixed value of 1 nm/s during the growth. The substrates were mounted on a rotating sample holder.

Proton beams of 3 and 7 MeV energies were produced by the PL7 model LINAC by ACCSYS-HITACHI [13]. At the output of the machine beamline a 50 μm thick kapton window was placed, which reduced the impinging protons energy to 2.23 and 6.65 MeV, respectively. The average beam current was 1 μA in 60 μs-long pulses at a repetition frequency of 50 Hz. The irradiation fluence covered the range of 10^{11}-10^{15} p/cm^2 by varying the total number of pulses delivered to different LiF samples.

LiF films were irradiated in air at RT in two different mounting geometries: perpendicularly to the proton beam for the detection of the transversal spatial distribution of the proton beam and parallel to the direction of the impinging protons, in order to reveal the Bragg peak position. After exposure, the stored images were read by the fluorescence microscope Nikon Eclipse 80-i C1, equipped with a Hg lamp. The blue emission of the Hg lamp, peaking at 434 nm, was optically filtered in order to simultaneously excite the PL of the F_2 and F_3^+ CCs and an Andor Neo s-CMOS camera was used to acquire the PL images with an 11-bit dynamic range. The Nikon software NIS Elements 4.20 was used to control the optical image acquisition system and the PL image analysis was performed by ImageJ software.

The PL spectra of proton-irradiated LiF films grown on glass were measured at RT by pumping in a continuous wave regime with the 457.9 nm line of an Argon laser, which allows to simultaneously excite the green and red emissions of F_3^+ and F_2 CCs. The PL signal was spectrally filtered by a monochromator and acquired by means of a photomultiplier with lock-in technique. The PL spectra were corrected for the instrumental calibration.

3. Results and Discussion

An important characteristic of the solid state LiF film radiation imaging detectors based on the PL of CCs is the possibility of storing information about the transverse proton beam intensity. Figure 1 shows the PL image of a 7 MeV proton beam stored in a LiF film ≅0.8 μm thick grown on a glass substrate. A quite well collimated proton beam is clearly observed. The formation of stable aggregate F_2 and F_3^+ electronic defects in LiF thin films grown on glass substrates was systematically

investigated for low-energy (nominally 3 and 7 MeV) proton beams, in a fluence range from 10^{11} to 10^{15} p/cm^2 [6] in order to study the PL optical response. The integrated CCs PL intensities, as carefully derived from all the fluorescence images, similar to those reported in figure 1, exposed at different irradiation times for both the proton energies, are reported in figure 2. Proton energy loss in the matter continuously increases with depth, reaching the maximum value about at the end of the implantation path, whose position is strongly dependent on the proton energies. Figure 2 shows that the integrated CCs PL signal is proportional to the proton fluence and a linear optical response is found up to a fluence value of 8 x 10^{13} p/cm^2, over which a plateau appears [6]. This behaviour is very similar for 3 and 7 MeV proton beams, although the PL signal is higher for the LiF film exposed at the lower energy at all the investigated fluence values. Such a behaviour can be explained by simulations performed using SRIM software [12]. The inset of figure 2 reports the linear energy transfer (LET) as a function of the proton implantation depth in LiF for 3 and 7 MeV proton beams calculated by SRIM. LET is continuously increasing with depth, reaching the maximum value (Bragg peak) almost at the end of the implantation path, which is higher than the typical thickness of the used LiF films. In LiF films, due to their limited thickness (only 0.8 μm), LET can be considered as constant and only a very small fraction of the total proton energy is lost in them, the rest being deposited in the glass substrate. As shown in the inset of figure 2, the initial LET is lower for 7 MeV protons (12 keV/μm) than for 3 MeV protons (28.4 keV/μm), which is consistent with the lower PL intensity of 7 MeV proton irradiated LiF films.

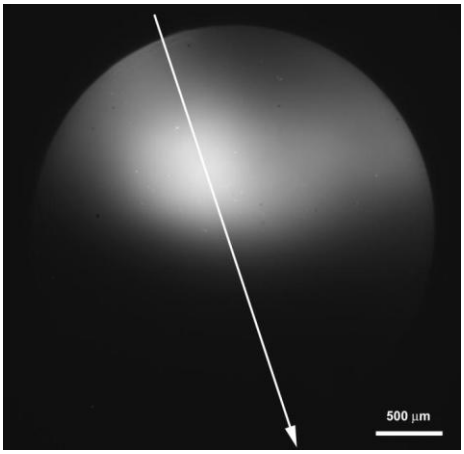

Figure 1 PL optical image of a 7 MeV proton beam transversal section, after passing through a circular aperture, stored by F_2 and F_3^+ colour centres in a LiF film 0.8 μm thick thermally evaporated on a glass substrate.

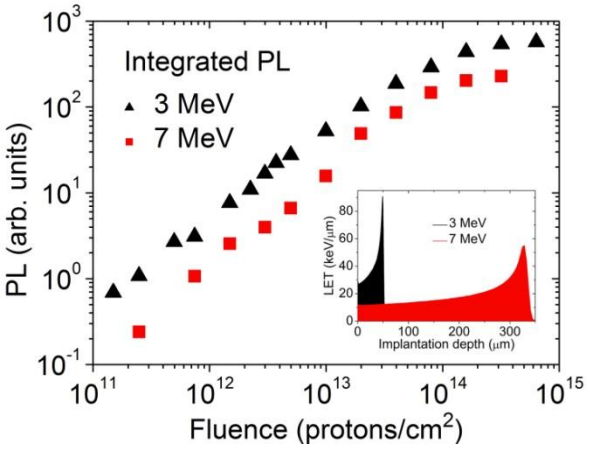

Figure 2. Integrated visible PL signal as a function of the proton fluence in LiF films grown on a glass substrate irradiated by 3 and 7 MeV proton beams as derived from optical images. Inset: SRIM simulation of LET for 3 and 7 MeV proton beams in LiF (see text for details).

In figure 3 the PL intensity profile along the white arrow traced in figure 1 is plotted. Due to the presence of a circular pinhole before the film surface, it is interesting to note that the PL signal value measured outside the pinhole diameter, in the left side of figure 3, corresponding to the "zero" value from a not-exposed film area, is comparable with the signal measured in the not-irradiated area of the exposed LiF film, in the right side of figure 3, outside of the quite well collimated proton beam. This behaviour indicates that the quite good optical quality of the transparent LiF film thermally evaporated on glass does not introduce significant noise contribution in the fluorescence image outside of the proton irradiated area. By comparison, bare glass substrates, irradiated in similar conditions, showed no PL signal in the same measurement conditions, although some darkening was observed in white light. The PL intensities measured by the fluorescence optical microscope were attributed to the local

formation of stable F_2 and F_3^+ CCs, as confirmed by PL spectra [5,6]. As example, the PL spectrum of a LiF film irradiated by 7 MeV protons at a fluence value of $2.4x10^{12}$ p/cm^2 is shown in figure 4 as a function of the energy. Its best fit shows that it consists of the superposition of two broad Gaussian emission bands, peaked at around 541 nm and 678 nm, ascribed to F_3^+ and F_2 centres, respectively [3,4]. These emission bands in the PL spectra of proton irradiated LiF films exhibit the same spectral features (peak position and half-width) of irradiated LiF crystals [4] and remained unchanged in the investigated fluence range (not shown).

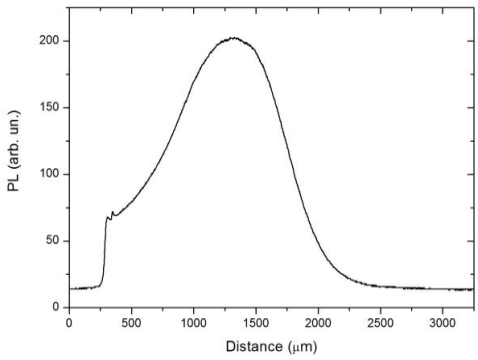

Figure 3. PL intensity profile along the white arrow of figure 1.

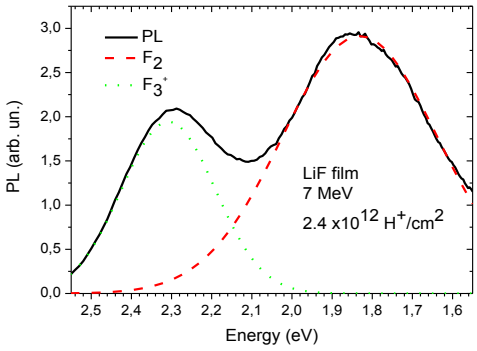

Figure 4. RT laser induced (457.9 nm) PL spectra of a LiF films 0.8 μm thick grown on a glass substrate and irradiated by a 7 MeV proton beam. The F_2 and F_3^+ CCs Gaussian bands obtained from its best fit are also shown.

Figure 5 shows the PL image of a 0.8 μm thick LiF film grown on Si(100) substrate, irradiated by the 7 MeV proton beam at a fluence of $1.6x10^{13}$ p/cm^2. The spectrally integrated PL emitted by radiation-induced F_2 and F_3^+ CCs, whose local concentrations are proportional to the energy deposited by protons in LiF, exhibits a strong increase at a distance from the cleaved edge of the film, whose amount depends on the proton beam energy. Below saturation, the PL signal is proportional to the local defects concentrations and the strong increase appears to be related to the Bragg peak position. Figure 6 shows the PL intensity profile acquired along the direction perpendicular to the film edge obtained by image analysis of the portion of figure 5 reported below in figure 6.

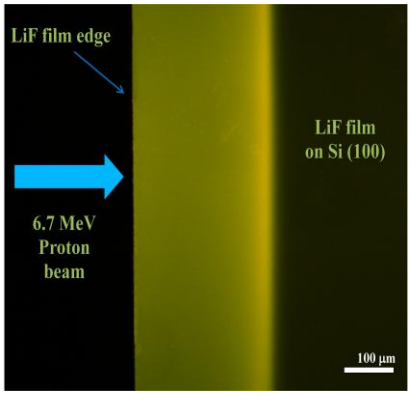

Figure 5. PL image of the top surface of a 0.8 μm thick LiF film grown on a Si(100) substrate, irradiated by a 7 MeV proton beam after cleavage and acquired by the fluorescence microscope.

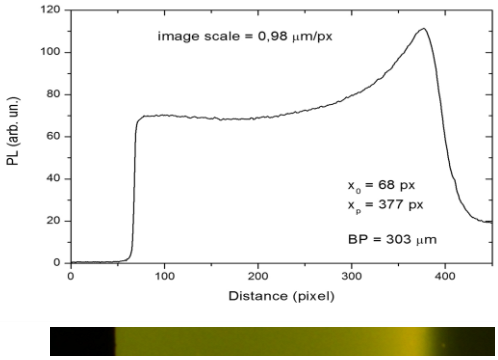

Figure 6. PL intensity profile acquired along the direction perpendicular to the film edge obtained by image analysis of the portion of figure 5 reported in the inset below.

Radiation induced defects are produced inside a thin layered volume, whose extension is comparable with protons implantation depth, within which they lose all their energy, and a maximum is experimentally found at a distance of ~ 303 μm. This value is comparable with the value found in LiF bulk at 295 μm, according to simulations performed by SRIM [12]. Although the good qualitative agreement, it should be also taken into account that the polycrystalline nature of LiF thin films could imply a reduced density of the LiF films, which can be considered as an aggregate of grains with air interstices [5,8,14].

From an independent estimate, obtained by optical reflectance spectra (not shown), a mean value of 2.609 g/cm^3 was derived. Figure 7 shows Bragg peak position depth values as a function of the proton energy as obtained from the SRIM simulation for a LiF film with the reduced density. The energy corresponding to the distance of 303 μm is too high with respect to the nominal one, whose nominal spread is only +/- 100 keV. On the other hand, it should be highlighted that the Bragg peak depth is extremely sensitive to the material density, as can be inferred from figure 8, where the LET values obtained from SRIM simulation at the effective energy of the impinging protons is shown for several LiF material densities, including bulk, and directly compared with the experimental PL depth profile directly obtained from figure 6.

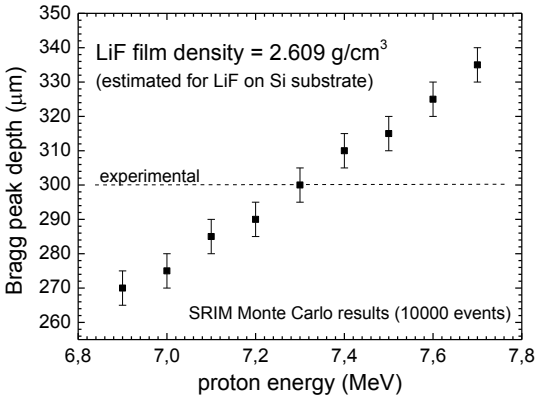

Figure 7. Bragg peak position as a function of the proton energy as obtained from accurate SRIM simulation for a LiF film of density 2.609 g/cm^3.

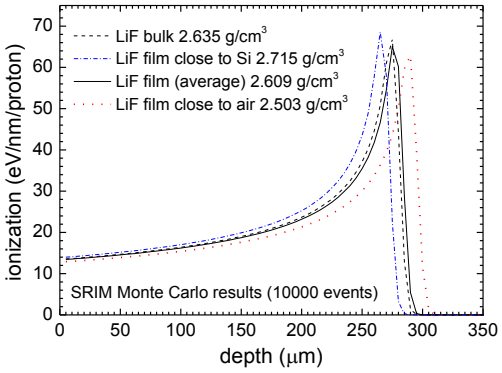

Figure 8. LET values obtained from accurate SRIM simulation for several LiF material densities, including bulk crystals, compared with the experimental PL depth profile in figure 6.

The measured depth at the maximum is higher of all the simulated values and eventually is compatible with a reduced density of 90.5%, which corresponds to 9.5% of voids in the films. However other phenomena, apart the polycrystalline nature of the used LiF samples, can affect the obtained results, among them irregularities in the cleaved edge, as well as PL scattering and image spatial resolution in the optical reading. Moreover, phenomena of diffusion and agglomeration of F CCs are expected to modify the defect profiles with respect to electronic energy loss in LiF crystals [11].

Saturation effects in the CCs PL response as a function of fluence (see figure 2) are responsible for the reduced differences between the PL values measured at the initial depth and on the maximum in the investigated conditions. Other complex phenomena, related to the high proton energy release at the end of the track (nuclear collision) cannot be excluded.

4. Conclusions

Although the PL signal of CCs in proton-irradiated LiF films is at least one order of magnitude lower than in crystals [6] because only a small fraction of the total proton energy is released in it, the rest being deposited in the substrate, optically transparent thin LiF films are able to store information about the proton beam intensity (high sensitivity) with a high spatial resolution (smooth profile) and to reveal even subtle intensity differences (high dynamic range). Despite of their low thickness, at high proton fluencies, 2-D accumulated transversal spatial distributions were carefully measured by reading the latent two-dimensional (2-D) fluorescence images stored in the LiF thin films by local formation of aggregate F_2 and F_3^+ CCs broad-band visible light-emitting defects with an optical microscope under blue lamp excitation. The same reading technique was used to obtain the PL profiles along the proton trajectory, by using cleaved LiF films grown on Si(100). A view of Bragg's profile was experimentally obtained, in qualitative agreement with SRIM simulation and further refinements and experiments are under way.

All the presented results are very encouraging for advanced dose diagnostics of proton beams at high spatial resolution with LiF film detectors based on the visible PL of radiation-induced CCs.

Acknowledgments

Research carried out within the TOP-IMPLART (Oncological Therapy with Protons - Intensity Modulated Proton Linear Accelerator for RadioTherapy) project, funded by Regione Lazio, Italy.

References

[1] Montereali R M, Bonfigli F, Piccinini M, Nichelatti E, Vincenti M A 2016 *J. Lumin.* **170** 761
[2] Baldacchini G et al. 2005 *Rev. Sci. Instrum.* **76** 113104_1
[3] Nahum J and Wiegand D A 1967 *Phys. Rev.* **154** 817
[4] Baldacchini G, De Nicola E, Montereali R M, Scacco A and Kalinov V 2000 *J. Phys. Chem. Solids* **61** 21
[5] Piccinini M, Ambrosini F, Ampollini A, Picardi L, Ronsivalle C, Bonfigli F, Libera S, Nichelatti E, Vincenti M A and Montereali R M 2015 *Appl. Phys. Lett.* **106** 261108
[6] Piccinini M, Ambrosini F, Ampollini A, Carpanese M, Picardi L, Ronsivalle C, Bonfigli F, Libera S, Vincenti M A and Montereali R M 2014 *J. Lumin.* **156** 170
[7] Agullo-Lopez F, Catlow C R A, Townsend P D 1988 *Point Defects in Materials* (London, Academic Press) p 56
[8] Montereali R M 2002 *Handbook of Thin Film Materials* vol 3, ed H S Nalwa (San Diego: Academic Press) chapter 7 pp 399-431
[9] Ronsivalle C et al. 2011 *Eur. Phys. J. Plus* **126** 7 68
[10] Abu-Hassan L H and Townsend P D 1986 *J. Phys. C, Solid State Phys.* **19** 99
[11] Perez A, Balanzat E and Dural J 1990 *Phys. Rev. B* **41** 7 3943
[12] Ziegler J F, Ziegler M D and Biersack J P 2010 *Nucl. Instrum. Meth. B* **268** 1818
[13] Ronsivalle C et al. 2015 *Eur. Phys. Lett.* **111** 14002
[14] Montecchi M, Montereali R M and Nichelatti E 2001 *Thin Solid Films* **396**, 264